Quantum monodromy in the two-centre problem

2003 J. Phys. A: Math. Gen. 36 L307

(http://iopscience.iop.org/0305-4470/36/20/103)

INSTITUTE OF PHYSICS PUBLISHING JOURNAL OF PHYSICS A: MATHEMATICAL AND GENERAL

J. Phys. A: Math. Gen. **36** (2003) L307–L314 PII: S0305-4470(03)59838-9

LETTER TO THE EDITOR

Quantum monodromy in the two-centre problem

H Waalkens[1,4], A Junge[2,4] and H R Dullin[3,4]

[1] School of Mathematics, Bristol University, University Walk, Bristol, BS8 1TW, UK
[2] Institute for Electromagnetic Compatibility, Technical University of Braunschweig, Schleinitzstr. 23, D-38106 Braunschweig, Germany
[3] Mathematical Sciences, Loughborough University, LE11 3TU, UK
[4] Institute of Theoretical Physics, Bremen University, PO Box 330 440, D-28334 Bremen, Germany

E-mail: H.Waalkens@bris.ac.uk

Received 20 February 2003
Published 7 May 2003
Online at stacks.iop.org/JPhysA/36/L307

Abstract

Using modern tools from the geometric theory of Hamiltonian systems it is shown that electronic excitations in diatoms which can be modelled by the two-centre problem exhibit a complicated case of classical and quantum monodromy. This means that there is an obstruction to the existence of global quantum numbers in these classically integrable systems. The symmetric case of H_2^+ and the asymmetric case of HHe^{++} are explicitly worked out. The asymmetric case has a non-local singularity causing monodromy. It coexists with a second singularity which is also present in the symmetric case. An interpretation of monodromy is given in terms of the caustics of invariant tori.

PACS numbers: 03.65.Sq, 05.45.−a, 31.10.+z

The two-centre problem represents an important integrable limiting case of the three-body problem. As such it has a long history dating back to Euler and Jacobi, see [1, 2] and the reference therein. The corresponding quantum system plays a similar fundamental role in molecular physics as the hydrogen atom in atomic physics. As a model for the simplest molecule H_2^+ the symmetric two-centre problem is a paradigm for chemical bonding, and it was first considered by Pauli in his doctoral thesis under the direction of Sommerfeld [3]. The separation of the Schrödinger equation was done in the 1930s [4], but their expansion method only captures the low lying Keplerian states. A systematic semiclassical approach was given by Strand and Reinhardt [5] and only very recently, an improvement of their results including consideration of the asymmetric case was presented in [6]. Besides its obvious role in molecular physics the importance of the two-centre problem extends to aspects of two electron atoms [7], ion–atom scattering [8] and elementary particle physics [9]. Despite the long and outstanding history of the two-centre problem it has not been recognized before that the system exhibits classical and quantum monodromy. Monodromy describes the effect of a global twisting of a family of invariant tori parametrized by a circle of regular values of the

energy–momentum map of the integrable system. This leads to topological obstructions to the definition of single-valued smooth action variables as shown by Duistermaat [10]. A quantum mechanical consequence of monodromy is the non-uniqueness of quantum numbers, as first reported by Cushman and Duistermaat [11] for the spherical pendulum, and later rigorously proved in [12]. In recent years the concept of monodromy has given insight into the spectra of prominent quantum systems as, e.g., the bending progressions of quasi-linear molecules [13], the spectrum of the hydrogen atom in the crossed fields configuration [14], rearrangements of bands in systems with coupled angular momenta [15] and vibrational spectra of Bose condensates [16].

1. The two-centre problem

The two-centre problem (TCP) describes the motion of a test particle in the field of two fixed attracting centres. In the diatomic interpretation the two-centres are two nuclei with charge $Z_i e$ attracting a single electron of charge $-e$; the distance between the nuclei is considered fixed at $2d$ in the Born–Oppenheimer approximation. We choose d, m_e and $(m_e d^3/e^2(Z_1+Z_2))^{1/2}$ as unit of length, mass and time, respectively. With the z-axis along the line connecting the fixed centres the Hamiltonian in Euclidean coordinates is

$$H = \frac{\mathbf{p}^2}{2} - \frac{\mu_1}{r_+} - \frac{\mu_2}{r_-} \tag{1}$$

where $r_\pm^2 = x^2 + y^2 + (z \pm 1)^2$ and $\mu_1 = \mu_2 = 1/2$ for H_2^+ or $\mu_2 = 2\mu_1 = 2/3$ for HHe^{++}. Due to rotational symmetry about the z-axis $L_z = xp_y - yp_x$ is conserved. The non-trivial constant of motion is obtained from the separation constant $G = \Omega + H$ [17] where, with $\mathbf{L} = \mathbf{r} \times \mathbf{p}$ being the angular momentum, Ω reads

$$2\Omega = \mathbf{L}^2 - \left(p_x^2 + p_y^2\right) + 2(z+1)\frac{\mu_1}{r_+} - 2(z-1)\frac{\mu_2}{r_-}. \tag{2}$$

The constants of motion H, G, L_z are in involution and independent almost everywhere, and where independent the Liouville–Arnold theorem [18] guarantees the existence of action angle variables for the invariant 3-tori of bounded motion. We denote the values of the constants of motion by h, g and l.

The TCP can be separated in prolate ellipsoidal coordinates

$$\phi = \arctan(y/x) \qquad \eta = (r_+ - r_-)/2 \qquad \xi = (r_+ + r_-)/2 \qquad (-1 \leqslant \eta \leqslant 1 \leqslant \xi). \tag{3}$$

The separation makes each conjugate momentum a function of only its respective coordinate and the values of the constants of motion (h, g, l) that fix the 3-torus. They are

$$p_\phi = L_z = l \qquad p_\eta^2 = P_-(\eta)/(1-\eta^2)^2 \qquad p_\xi^2 = P_+(\xi)/(1-\xi^2)^2 \tag{4}$$

where

$$P_\pm(\zeta) = 2(\zeta^2 - 1)(h\zeta^2 + (\mu_2 \pm \mu_1)\zeta - g) - l^2. \tag{5}$$

2. Caustics

Most of the structure of the problem is contained in the polynomials $P_\pm$. Their roots delimit the intervals of real momenta in (4), and the occurrence of double roots corresponds to bifurcations of tori. In the generic case $l \neq 0$ a regular value (h, g, l) has a single torus (T_P) or two tori (T_S) in its preimage in phase space. The corresponding caustics which are shown in figure 1(a) are composed of coordinate surfaces of the separating coordinates (ϕ, η, ξ). For $l = 0$ the

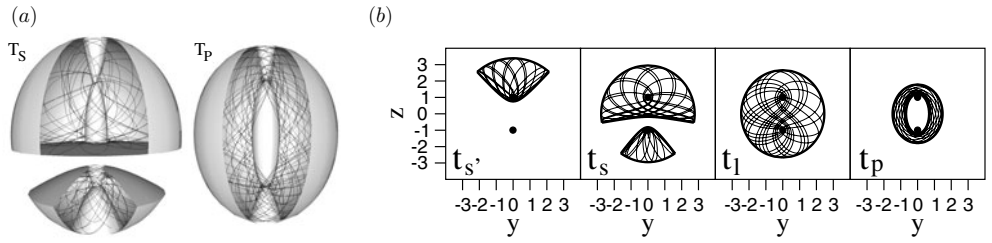

Figure 1. (*a*) Caustics of generic tori in the asymmetric TCP with $l \neq 0$. The stronger centre is at the top. (*b*) Caustics of 2-tori in the planar asymmetric TCP. Following the notation in [1], s, l and p refer to satellite, lemniscate and planetary-type motion, respectively. In the symmetric TCP $t_{s'}$ does not exist and the others are symmetric.

3-tori become resonant and are foliated by invariant 2-tori of planar motions. These 2-tori have three different types of caustics in the symmetric case and four different types of caustics in the asymmetric case. They are presented in figure 1(*b*). As $l \to 0$, the generic caustic T_P gives rise to the three topologically different caustics $t_{s'}$, t_l and t_p for the asymmetric TCP, and to the two caustics t_l and t_p for the symmetric case.

We will see that monodromy in the TCP can be explained by the change of caustics at $l = 0$. The symmetry axis connecting the two centres can only be reached by the electron when the conserved angular momentum vanishes. Due to the singularity in the coordinate system this single line in physical space consists of the three segments $\xi = 1$ (between the nuclei), and $\eta = \pm 1$ (above/below the nuclei) in the ellipsoidal coordinates. Monodromy will be determined by the number of singular segments visited by the motion in configuration space, see figure 1(*b*). For the ξ-coordinate this is 0 for t_p, 1 otherwise, while for the η-coordinate it is 1 for $t_{s'}$ and 2 otherwise.

3. Bifurcation diagrams

The relation between the type of motion and the value of the constants of motion is best described in terms of bifurcation diagrams. The bifurcation diagram is the set of critical values of the energy–momentum map given by (H, G, L_z). At a critical point the constants of motion are not independent and the Liouville–Arnold theorem does not apply. One can check that the double roots of $P_\pm$ in the physical range $-1 \leqslant \eta \leqslant 1 \leqslant \xi$ give critical points of the energy–momentum map. It turns out that the complete bifurcation diagram can be conveniently parametrized by the location of the double roots of $P_\pm$.

We illustrate the bifurcation diagram by showing sections of constant energy, see figure 2 for the symmetric TCP and figure 3 for the asymmetric TCP. At critical energies bifurcations occur and the structure of the sections changes. The Hamiltonian Hopf bifurcations at $h = -(\mu_1 + \mu_2)/2 = -1/2$, in both the symmetric and the asymmetric TCP, creates the planetary-type motion t_p; the isolated periodic orbit bouncing between the two nuclei becomes unstable. This orbit corresponds to the isolated points F in figure 2 and F_1 in figure 3. Another Hopf bifurcation in the asymmetric case, at $h = -|\mu_1 - \mu_2|/2$, destroys the single nucleus motion T_S and renders unstable the orbit that is deflected from the weakly charged nucleus to the outside (the point F_2 in figure 3). Note that even before this bifurcation takes place the 'kite shaped' region T_S at energies h_3 and h_4 in figure 3 is isolated in the sense that it can be encircled by a loop of non-critical values in T_P. The existence of loops that cannot

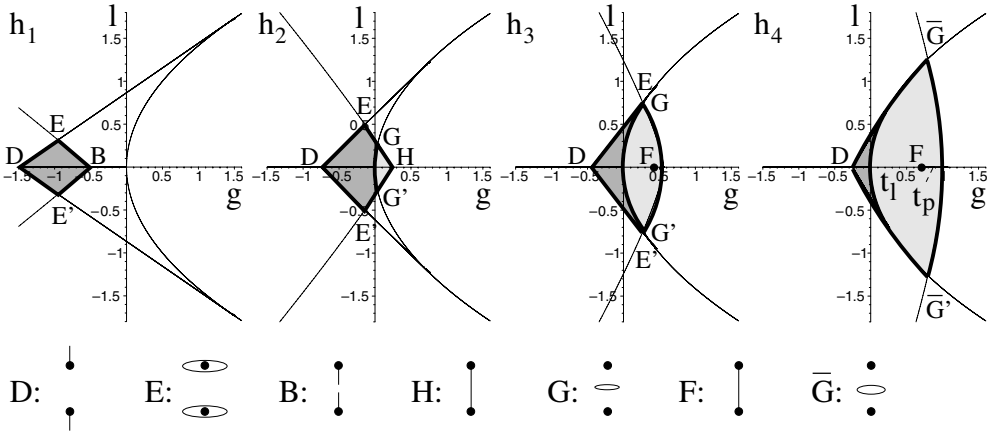

Figure 2. Bifurcation diagrams (thick lines) of the symmetric TCP for representative energies $h_1 < h_2 < h_3 < h_4 < 0$. To each point in the light or dark grey regions there corresponds a single torus (T_P) or two tori (T_S) in phase space, respectively. The corners represent the periodic orbits shown in the lower panel. D, E, B, H and $\overline{G}$ are stable and G and F are unstable. The primes denote the respective time reversed periodic orbits. Resonant tori of type t_l and t_p are on the ($l = 0$)-axis to the left and right of the isolated point F, respectively, as shown for $H = h_4$.

be contracted without intersecting the bifurcation diagram is indicative of the existence of monodromy.

4. Actions and monodromy

Let us concentrate on the family of invariant tori of type T_P represented by the light grey regions in figures 2 and 3. Since there is a separating coordinate system the natural choice of action variables is

$$\mathbf{I} = (L_z, I_\eta, I_\xi)^t = \left(l, \frac{1}{2\pi} \oint_{\gamma_\eta} p_\eta \, \mathrm{d}\eta, \frac{1}{2\pi} \oint_{\gamma_\xi} p_\xi \, \mathrm{d}\xi \right)^t . \tag{6}$$

With ζ representing η or ξ the projections of the closed paths γ_ζ to configuration space are coordinate lines of the separating coordinate system.

Let us first show that the *natural actions* $\mathbf{I}$ are continuous but not differentiable at $l = 0$. To see this note at first that l enters the polynomials $P_\pm(\zeta)$ in (5) quadratically. Hence, the discrete symmetry w.r.t. reversing angular momentum gives

$$\mathbf{I}(l) = \mathbf{R}\mathbf{I}(-l) \qquad \mathbf{R} = \mathrm{diag}(-1, 1, 1). \tag{7}$$

The matrix $\mathbf{R}$ contains the signs indicating that the first component of $\mathbf{I}(l)$ is odd, while the actions I_ζ are even in l. Hence, if the action components I_ζ were differentiable w.r.t. l at $l = 0$ the partial derivatives $\partial I_\zeta / \partial l$ would vanish at $l = 0$. By a deformation of the paths for the integration of $\partial I_\zeta / \partial l$ in the complex plane, $\partial I_\zeta / \partial l$ can be calculated in the limit $l \to 0+$ from the residues of the integrand $\partial / \partial l \sqrt{P_\pm(\zeta)}/(1 - \zeta^2)$ augmented by information about which of the singular points $\zeta = \pm 1$ are encountered. A careful choice of the branch of $\sqrt{P_\pm}$ yields the result that each singularity contributes the residue $-1/2$, i.e. the slopes $\lim_{l \to 0+} \partial I_\zeta / \partial l$ are simply given by $-1/2$ times the number of singular coordinate segments involved.

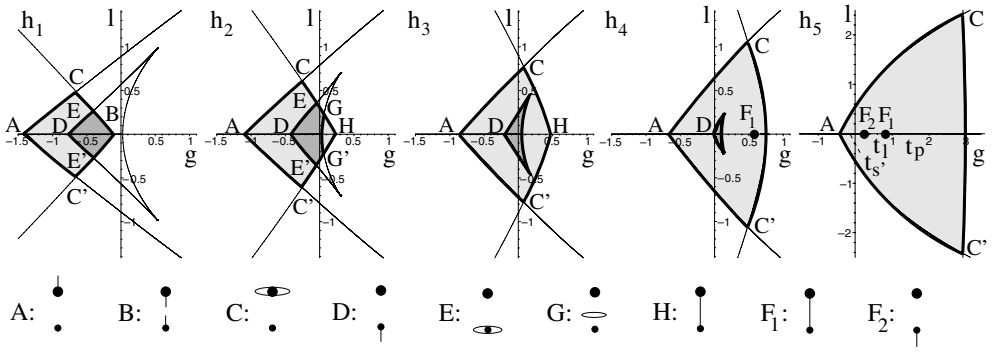

Figure 3. Analogue of figure 2 for the asymmetric TCP. The periodic orbits A, B, C, D, E and H are stable, G, F_1 and F_2 are unstable. The location of the segments $t_{s'}$, t_l and t_p of the $(l = 0)$-axis is shown for $H = h_5$.

This number can be read off from the caustics and we already determined it above. In this way we obtain

$$\lim_{l\to 0+}\left(\frac{\partial I_\eta}{\partial l},\frac{\partial I_\xi}{\partial l}\right)=\begin{cases}(-1/2,-1/2) & t_{s'}\\ (-1,-1/2) & t_l\\ (-1,0) & t_p.\end{cases} \tag{8}$$

Note that the tori at $l = 0$ satisfy the resonance condition $\mathbf{m}\cdot\omega = 0$ with the rational vector $\mathbf{m} = \lim_{l\to 0+}(1, \partial I_\eta/\partial l, \partial I_\xi/\partial l)$.

From the Liouville–Arnold theorem we know that, locally, there exist smooth actions for regular values of the energy–momentum map. To find them we retain the actions $\mathbf{I}$ for $l \geqslant 0$ and define new actions for $l < 0$. Since actions are defined up to unimodular transformations locally smooth actions can be obtained from

$$\mathbf{J}=\begin{cases}\mathbf{I} & l\geqslant 0\\ \mathbf{MI} & l<0\end{cases} \tag{9}$$

where $\mathbf{M}\in SL(3,\mathbb{Z})$ remains to be determined. Since the *natural actions* $\mathbf{I}$ are continuous at $l = 0$, the matrix $\mathbf{M}$ can differ from the identity only in its first column for which we write $(1, m_\eta, m_\xi)^t$. The integers m_ζ are obtained by equating the left- and right-hand derivatives of $\mathbf{J}$,

$$\lim_{l\to 0+}\frac{\partial I_\zeta}{\partial l}=\lim_{l\to 0-}\frac{\partial J_\zeta}{\partial l}\quad\Leftrightarrow\quad m_\zeta = 2\lim_{l\to 0+}\frac{I_\zeta}{\partial l}. \tag{10}$$

As we have already seen, the limits $\lim_{l\to 0+}\partial I_\zeta/\partial l$ depend on whether we have $t_{s'}$, t_l or t_p on $l = 0$. This way we obtain the three matrices

$$M_{s'}=\begin{pmatrix}1&0&0\\-1&1&0\\-1&0&1\end{pmatrix}\qquad M_l=\begin{pmatrix}1&0&0\\-2&1&0\\-1&0&1\end{pmatrix}\qquad M_p=\begin{pmatrix}1&0&0\\-2&1&0\\0&0&1\end{pmatrix}. \tag{11}$$

Monodromy describes the change of smooth actions along a closed loop of regular values of the constants of motions. If the loop is contractible there is no change. In the TCP the isolated singularities that can prevent this are located on $l = 0$. Encircling them we cross $l = 0$ twice in regions with different $l = 0$ caustics. In the symmetric case a closed loop about F in figure 2 crosses t_l and t_p. In the asymmetric case we cross $t_{s'}$ and t_l for a loop about F_1 and t_l and t_p for a loop about F_2 or the isolated kite shaped region T_S in figure 3. For

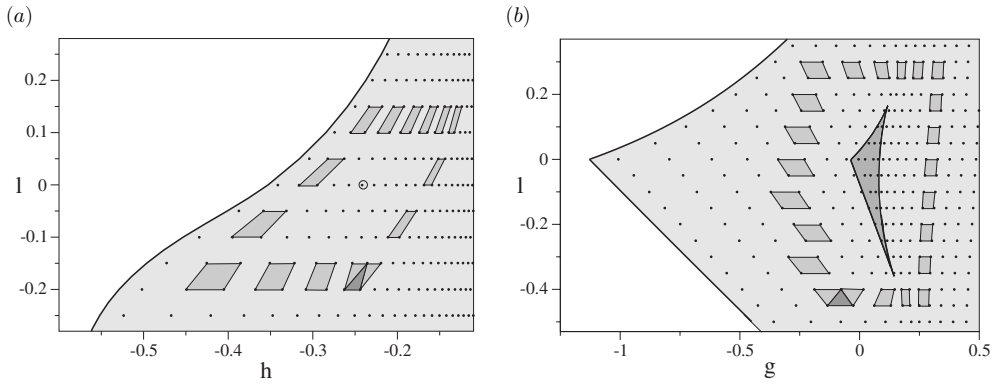

Figure 4. (*a*) Surface of eigenvalues with $n_\eta = 26$ in the symmetric TCP. The circle marks the intersection with the isolated line F of the bifurcation diagram in figure 2. Monodromy is illustrated by transporting a quantum cell around the singular point. (*b*) Surface of eigenvalues with $n_\xi = 11$ in the asymmetric TCP. Monodromy around a non-local singularity is illustrated.

the anticlockwise traversal of a loop crossing t_a and t_b with (a, b) any pair from $\{s', l, p\}$ the monodromy matrix $\mathbf{M}_{ab}$ describing the unimodular change of the smooth actions $\mathbf{J}$ of (9) is

$$\mathbf{M}_{ab} = (\mathbf{M}_b\mathbf{R})^{-1}\mathbf{M}_a\mathbf{R} = \mathbf{M}_b\mathbf{R}\mathbf{M}_a\mathbf{R} = \mathbf{M}_b\mathbf{M}_a^{-1} \tag{12}$$

where we used that $\mathbf{R}$ is a reversor for each of the $\mathbf{M}_a$ of (11), i.e. $\mathbf{R}\mathbf{M}_a\mathbf{R} = \mathbf{M}_a^{-1}$, $a = s', l, p$. This way we obtain the monodromy matrices

$$\mathbf{M}_{s'l} = \begin{pmatrix} 1 & 0 & 0 \\ -1 & 1 & 0 \\ 0 & 0 & 1 \end{pmatrix} \qquad \mathbf{M}_{lp} = \begin{pmatrix} 1 & 0 & 0 \\ 0 & 1 & 0 \\ 1 & 0 & 1 \end{pmatrix}. \tag{13}$$

The fact that they differ from the identity matrix proves the presence of monodromy, i.e. the smooth continuation of actions leads to multivalued functions.

5. Quantum monodromy

The quantum mechanical two-centre problem is described by three commuting operators $\hat{H}$, $\hat{G}$ and $\hat{L}_z$ which are related to the constants of motion H, G and L_z by the correspondence principle [19]. The implications of monodromy on the joint spectrum of these operators, which for the bound quantum states is a point set in $\mathbb{R}^3(h, g, l)$, can be described semiclassically. In terms of the natural actions the EBK quantization conditions are $\mathbf{I} = \hbar(\mathbf{n}+\alpha/4)$ with quantum numbers $\boldsymbol{n}$. The vector of Maslov indices is $\alpha = (0, 2, 2)^t$ for *all* 3-tori of the TCP.

In order to illustrate the quantum monodromy we choose certain subsets of states with eigenvalues located on two-dimensional surfaces in $\mathbb{R}^3(h, g, l)$ which intersect the isolated parts of the bifurcation diagram transversally. The surface of quantum states in the symmetric TCP shown in figure 4(*a*) is defined by $J_\eta = \hbar(n_\eta + 1/2)$ with a constant $n_\eta \in \mathbb{N}$. The quantum numbers of this subset of states are invariant under $\mathbf{M}_p$, $\mathbf{M}_l$, $\mathbf{M}_{lp}$ defined in (11) and (13). As expected from the monodromy matrix $\mathbf{M}_{lp}$ a cell of the eigenvalue lattice transported on a closed loop about the isolated point F returns sheared by one lattice site. Due to this defect of the eigenvalue lattice there are only two 'good' or single-valued quantum numbers, the angular momentum quantum number n_ϕ and n_η, to label states which classically correspond to tori of type T_P. The situation about the isolated point F_1 of the asymmetric TCP is similar and we

omit the presentation of a separate figure. Even more spectacular is the defect of the eigenvalue lattice of the asymmetric TCP shown in figure 4(*b*). The eigenvalue surface there is given by $J_\xi = \hbar(n_\xi + 1/2)$ with a constant $n_\xi \in \mathbb{N}$. It is invariant under $\mathbf{M}_{s'}$, $\mathbf{M}_l$, $\mathbf{M}_{s'l}$ from (11) and (13). In accordance with the monodromy matrix $\mathbf{M}_{s'l}$ a lattice cell returns also sheared by one lattice site when transported about the non-local singularity. Since the eigenvalue lattice of the asymmetric TCP has two defects with different invariant lattice planes there is no further 'good' global quantum number besides the angular momentum quantum number.

6. Conclusions

In this letter we reported on classical and quantum monodromy in the two-centre problem which is a highly interesting result because of the special importance of the two-centre problem in physics on the one hand and the particularly interesting variant of monodromy exhibited by the two-centre problem on the other.

Monodromy is well understood in two degrees of freedom where its simplest form is related to a focus–focus singularity and the monodromy matrix is of the form $(1, n; 0, 1)$ when the corresponding separatrix connects $n \geqslant 1$ focus–focus critical points [20]. The monodromy in the symmetric two-centre problem where the source of monodromy is a codimension 2 singularity is similar. The 3×3 monodromy matrix has only a single off-diagonal entry and in principle a reduction to the two degree of freedom case should be possible. In contrast to that, there are two sources of monodromy in the asymmetric two-centre problem of which one is of non-local nature. The corresponding 3×3 matrices have only a single non-trivial off-diagonal entry. But since the non-trivial entries appear at different positions within the monodromy matrices they act on different action components and for a complete picture it is necessary to analyse the full three degree of freedom system.

In our calculations we kept the distance between the nuclei fixed. This is an unrealistic simplification for single electron diatoms. Hence, H_2^+ and HHe^{++} should be considered as symbols for systems that can be modelled by the TCP, as e.g., Rydberg states in polyelectronic molecules where the bonding is maintained by the non-excited electrons. In figures 4(*a*) and 4(*b*) we chose $d = m = e^2 = 1$ and $\hbar = 1/20$ to obtain a sufficiently high density of states for the matter of representation. The experimental observation of monodromy requires excitation to energies $h \in (-(\mu_1 + \mu_2)/2, 0)$, or to $h \in [-0.553, -1/6)$ for the special monodromy in the case of HHe^{++}. Many details of this work will be represented in a forthcoming paper [21].

Acknowledgments

We are grateful to Peter H Richter for his constructive comments. This research was partially supported by the European Research Training Network 'MASIE' (HPRN-CT-2000-00113) and the Deutsche Forschungsgemeinschaft (Wa 1590/1-1).

References

[1] Charlier C L 1902 *Die Mechanik des Himmels* (Leipzig: von Veit & Comp)
[2] Howard J E and Wilkerson T D 1995 *Phys. Rev.* A **52** 4471
[3] Pauli W 1922 *Ann. Phys., Lpz* **68** 177
[4] Jaffe G 1935 *Z. f. Phys.* **87** 535
Baber W G and Hasse H R 1935 *Cambridge Phil. Soc. Proc.* **31** 564
[5] Strand M P and Reinhardt W P 1979 *J. Chem. Phys.* **70** 3812
[6] Athavan N, Fröman P O, Fröman N and Lakshmanan M 2001 *J. Math. Phys.* **42** 5051
Athavan N, Fröman P O, Fröman N and Lakshmanan M 2001 *J. Math. Phys.* **42** 5077
Athavan N, Fröman P O, Fröman N and Lakshmanan M 2001 *J. Math. Phys.* **42** 5096

[7] Tanner G, Richter K and Rost J-M 2000 *Rev. Mod. Phys.* **72** 497
[8] Hatton G J, Chen J C Y, Ishihara T and Watson K M 1975 *Phys. Rev.* A **12** 1281
Piacentini R D and Salin A 1976 *J. Phys. B: At. Mol. Phys.* **7** 1666
Winter T G, Duncan M D and Lane N F 1977 *J. Phys. B: At. Mol. Phys.* **10** 285
[9] Ponomarev L I and Puzynina T P 1967 *Sov. Phys.–JETP* **25** 846
Ponomarev L I 1966 *Sov. J. Nucl. Phys.* **2** 160
[10] Duistermaat J J 1980 *Commun. Pure Appl. Math.* **33** 687
[11] Cushman R H and Duistermaat J J 1988 *Bull. Am. Math. Soc.* **19** 475
[12] Vu Ngoc S 1999 *Commun. Math. Phys.* **203** 465
[13] Child M S, Weston T and Tennyson J 1996 *Mol. Phys.* **96** 371
[14] Cushman R H and Sadovskii D A 1999 *Europhys. Lett.* **47** 1
Cushman R H and Sadovskii D A 2000 *Physica* D **142** 166
[15] Sadovskii D A and Zhilinskii B I 1999 *Phys. Lett.* A **256** 235
Grondin L, Sadovskii D A and Zhilinskii B I 2001 *Phys. Rev.* A **65** 012105
[16] Waalkens H 2002 *Europhys. Lett.* **58** 162
Waalkens H and Dullin H R 2002 *Ann. Phys., NY* **295** 81
[17] Coulson C A and Joseph A 1967 *Int. J. Quantum Chem.* **1** 337
[18] Arnold V I 1978 *Mathematical Methods of Classical Mechanics* (Heidelberg: Springer)
[19] Erikson H A and Hill E L 1949 *Phys. Rev.* **75** 29
[20] Zung Tien N 1997 *Diff. Geom. Appl.* **2** 123
[21] Waalkens H, Dullin H R and Richter P H 2003 to be published